Analysis of phase synchronization of coupled chaotic oscillators with empirical mode decomposition

A. Goska and A. Krawiecki
Faculty of Physics, Warsaw University of Technology, Koszykowa 75, PL-00-662 Warsaw, Poland
(Received 16 December 2005; revised manuscript received 14 March 2006; published 30 October 2006)

Empirical mode decomposition is investigated as a tool to determine the phase and frequency and to study phase synchronization between complex chaotic oscillators. Within this approach, the oscillator is characterized by a spectrum of frequencies corresponding to the empirical modes. First, the phase and frequency of the oscillators resulting from two well-known methods, based on modified variables and the Poincaré surface of section, are compared with those obtained using empirical mode decomposition. Next, for both parametrically and essentially different chaotic oscillators coupled as a drive-response system, transition to phase synchronization between corresponding empirical modes is investigated, defined as an adjustment of the mode frequencies of the response oscillator to those of the drive oscillator as the coupling is increased. In particular, anomalous and imperfect phase synchronization between modes is observed.

DOI: 10.1103/PhysRevE.74.046217 PACS number(s): 05.45.Xt, 05.45.Tp

I. INTRODUCTION

Recently, increasing interest in synchronization phenomena in periodic and chaotic oscillators has been observed [1,2]. Generally, synchronization means an adjustment of the states of the interacting systems. According to different types or levels of this adjustment, e.g., complete [3], lag [4], generalized [5], marginal [6], and phase synchronization (PS) [7,8] can be specified.

PS is a weak form of synchronization. It is characterized by an adjustment of phases, while amplitudes of the oscillations can remain uncorrelated [7]. However, phase can be unambiguously determined only for linear oscillators. Also in simple chaotic oscillators (e.g., Rössler system) the phase can be easily approximated due to the existence of a unique center of rotation [9,10]. However, for more complex chaotic oscillators (e.g., Lorenz [11], Chen [12], and Lü [13] systems) determining the phase is difficult. The main problem is to find the proper center and direction of rotation, because a set of saddle cycles, present in the chaotic state, introduces various rotation centers [14]. Thus there is no unique method to determine the phase in complex chaotic oscillators, and different definitions of the phase can be found [14–16]. Moreover, coupling between different chaotic systems can cause significant deformation of their attractors even in the case of simple chaotic oscillators, which also makes impossible defining the phase and studying PS on the basis of simple physical intuitions.

Chaotic time series can be decomposed into a finite sum of empirical modes, each with a unique center and direction of rotation, using a procedure called empirical mode decomposition (EMD) [17]. For each mode, the phase and instantaneous frequency can be unambiguously defined; though the latter can vary significantly in time, by definition the average frequency is decreased when going from lower to higher modes. In Ref. [18] the idea was put forward to use EMD to study PS bewteen coupled chaotic oscillators, or between periodic forcing and a chaotic oscillator. PS was defined as phase locking of the empirical modes of the response oscillator with corresponding modes of the drive oscillator, or directly with the periodic forcing. As examples, PS between parametrically different chaotic forced van der Pol oscillators and between electroencephalographic signals from different regions of the brain of an epileptic patient were investigated. In both cases phase diffusion, intermittent PS, and phase locking between corresponding modes, with close average frequencies, of the signals under study were observed.

The purpose of this paper is to further study EMD as a tool for determining the phase and frequency in complex chaotic oscillators and to compare systematically the results with those from other methods. The focus is to identify spectral components of the chaotic signal (e.g., empirical modes in the case of the EMD method) and to determine their frequencies. It is shown that both methods based on the Poincaré surface of section (PSS) and EMD reveal the presence of several intrinsic frequencies in the chaotic oscillations, but only in the latter case can both the phases and average frequencies of the empirical modes be unambiguously evaluated. Next, the transition to synchronization with increasing coupling strength between complex chaotic oscillators, both parametrically different and with topologically different attractors, is investigated by means of the EMD method. In contrast with Ref. [18], PS is defined as a process of merging of the frequencies of the corresponding modes in the time series of the two oscillators (frequency entrainment). Certain aspects of this PS—e.g., its relationship to the generalized synchronization [5] as well as anomalous [8,19] and imperfect [20] synchronization between modes—are briefly discussed.

II. PHASE AND INTRINSIC FREQUENCY SPECTRUM OF COMPLEX CHAOTIC OSCILLATORS

A. Lorenz system

The Lorenz system [11] $\dot{x}=\sigma(y-x)$, $\dot{y}=rx-y-xz$, $\dot{z}=xy-bz$ is a generic model to illustrate difficulties in defining the phase and frequency as well as in studying PS of complex chaotic oscillators. So far, phase has been defined for the Lorenz system using modified variables (MV's) [15] and

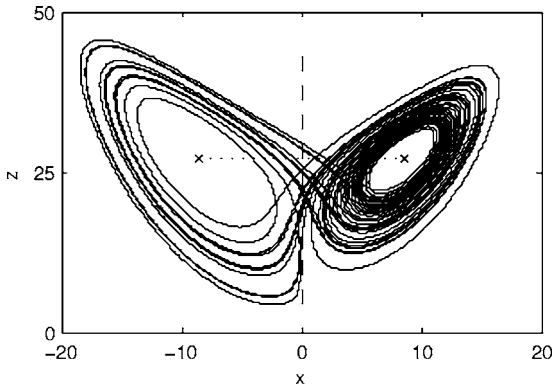

FIG. 1. Chaotic attractor of the Lorenz system with $\sigma=10$, $b=8/3$, and $r=28$. The lines show location of the Poincaré surfaces of section $z=r-1$ (dotted line) and $x=0$ (dashed line); the crosses show locations of the symmetric unstable foci.

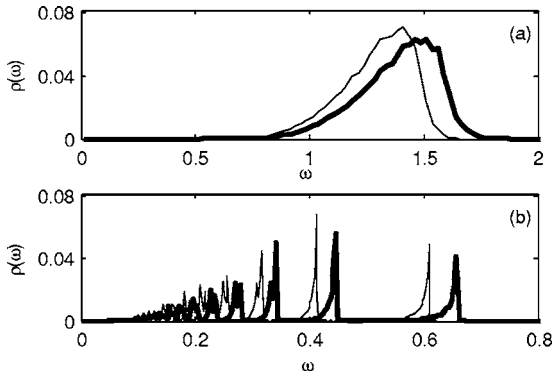

FIG. 2. Frequency distributions $\rho(\omega_i)$ of two different uncoupled Lorenz oscillators with $\sigma=10$, $b=8/3$, and $r=26$ (thin line) or $r=29$ (thick line). The surface of section is conditioned by (a) $z=r-1$ and (b) $x=0$.

PSS [14,16]. Recently, another definition of the phase using EMD has been introduced [21].

The main idea behind the MV method for the Lorenz system ($\sigma=10$, $r=28$, $b=8/3$, Fig. 1) is that its dynamics in the variables $u=\sqrt{x^2+y^2}, z$ looks like rotation around some center point $u_p=12$, $z_p=r-1$ [15]. Phase can be defined as $\phi=\arctan(\bar{z}/\bar{u})$, where $\bar{u}=u-u_p$, $\bar{z}=z-z_p$. Then, the instantaneous frequency is $\omega_{MV}=\frac{\dot{z}u\bar{u}-\bar{z}(x\dot{x}+y\dot{y})}{u(\bar{u}^2+\bar{z}^2)}$. Hence, the MV method yields a single frequency ω_{MV} (Table I).

The definition of phase in the PSS method is based on the geometric properties of the attractor. In this method a general assumption is made that every new rotation increases the phase by 2π. Rotation is understood as two consecutive intersections (from the same direction) of the surface of section by the phase trajectory. Certainly, this method provides no information about the evolution of the phase in time, since phase is defined with 2π accuracy; however, it is enough to determine the mean frequency. For this purpose, time intervals τ_i, $i=1,2,\ldots,N$, are counted between the intersections, and the system is characterized by a frequency distribution $\rho(\omega_i)$, where $\omega_i=\tau_i^{-1}$, and by the mean frequency $\omega_{PSS}=\int\rho(\omega)\omega d\omega$.

The outcome of the above-mentioned procedure depends on the choice of the surface of section. Let us first consider

TABLE I. Frequencies for two (uncoupled) Lorenz systems with $\sigma=10$, $b=8/3$, and r given in the table, obtained using different methods (for explanation of symbols see text).

	$r=29$, $\omega_{MV}=1.39$		$r=26$, $\omega_{MV}=1.30$	
j	$\omega_{PSS}^{(j)}$	$\omega_{EMD}^{(j)}$	$\omega_{PSS}^{(j)}$	$\omega_{EMD}^{(j)}$
0	1.36±0.03	1.70	1.27±0.03	1.60
1	0.64±0.02	0.84	0.59±0.02	0.77
2	0.44±0.01	0.54	0.40±0.01	0.51
3	0.33±0.01	0.29	0.31±0.01	0.28
4	0.27±0.01	0.17	0.25±0.01	0.16
5		0.10		0.09
6		0.05		0.05

the surface conditioned by $z=r-1$ (Fig. 1), with the intersections counted only when $dz/dt<0$ [16]. The resulting frequency distribution is unimodal [Fig. 2(a)] and the mean frequency $\omega_{PSS}^{(0)}$ agrees well with the frequency ω_{MV} from the MV method (Table I). However, with the surface set at $x=0$ (Fig. 1) and the intersections counted only when $dx/dt<0$, the frequency distribution exhibits multiple distinct peaks [Fig. 2(b)]. This means the presence of several spectral components in the system, which is thus characterized by an intrinsic frequency spectrum, with the frequencies $\omega_{PSS}^{(1)},\omega_{PSS}^{(2)},\ldots$ evaluated as averages over the separate maxima of the distribution. It can be seen that $\omega_{PSS}^{(0)}>\omega_{PSS}^{(1)}>\omega_{PSS}^{(2)}>\cdots$. This is so because $\omega_{PSS}^{(0)}$ results mainly from fast rotations of the trajectory around symmetric unstable foci (Fig. 1), while $\omega_{PSS}^{(j)}$, $j=1,2,\ldots$, are related to slower jumps between the two symmetric parts of the attractor with $x<0$ and $x>0$. Moreover, each jump can occur after the trajectory performs one, two, or more rotations around one of the unstable foci, which explains the multiple peaks of the frequency distribution in Fig. 2(b).

EMD is based solely on the chaotic signal under study and does not require any knowledge of the geometry of the attractor. Generally speaking, it results in the decomposition of a given signal $x(t)$ into a number of intrinsic modes $C_k(t)$, $k=0,1,\ldots,L$, each with its proper center and direction of rotation [21] (for details of the method see Ref. [17]). This is achieved by means of the following iterative procedure. In order to obtain $C_k(t)$ an input signal $\tilde{x}_k(t)$ is needed, which depends on the previous $k-1$ iterations of the procedure; to start the EMD, $\tilde{x}_0(t)=x(t)$ is assumed. In the first step, two smooth splines $\tilde{x}_{k,min}(t)$ and $\tilde{x}_{k,max}(t)$ connecting all the minima and all the maxima of $\tilde{x}_k(t)$, respectively, are constructed. In the second step, the mean $m_k(t)=[\tilde{x}_{k,max}(t)+\tilde{x}_{k,min}(t)]/2$ and the difference $\Delta\tilde{x}_k(t)=\tilde{x}_k(t)-m_k(t)$ are evaluated. If $\Delta\tilde{x}_k(t)$ corresponds to a proper rotation, the empirical mode is assumed as $C_k(t)=\Delta\tilde{x}_k(t)$; if not, the two above-mentioned steps are iterated with the input signal defined as $\tilde{x}_k(t)=\Delta\tilde{x}_k(t)$ until the resulting signal is a proper rotation. In practice, the signal is considered to be a proper rotation if a number of its maxima, minima, and zero crossings differs at most by 1 and if its mean $m_k(t)$ is close to 0.

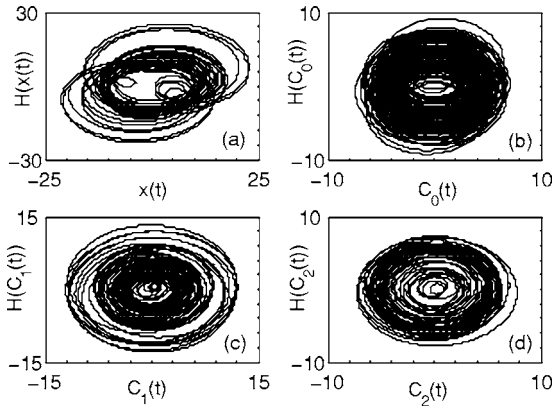

FIG. 3. (a) The original signal $x(t)$ and its Hilbert transform $H(x(t))$ from the Lorenz system with $\sigma=10$, $b=8/3$, and $r=28$. (b)–(d) The empirical modes $C_k(t)$ and their Hilbert transforms $H(C_k(t))$, $k=0,1,2$, from the Lorenz system.

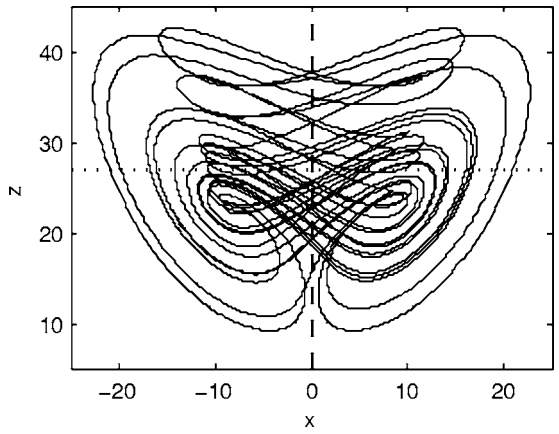

FIG. 4. Chaotic attractor of the Chen system with $\sigma=35$, $b=3$, and $r=28$. The lines show location of the Poincaré surfaces of section $z=r-1$ (dotted line) and $x=0$ (dashed line).

The parameters determining when to stop this iteration process are assumed as in Ref. [22]: the so-called evaluation function

$$\sigma_k(t) = |m_k(t)/a_k(t)|,$$

where

$$a_k(t) = [\tilde{x}_{k,max}(t) - \tilde{x}_{k,min}(t)]/2,$$

must fulfill the condition $\sigma_k < \theta_1$ for some prescribed fraction $(1-\alpha)$ of the total signal duration, while $\sigma_k < \theta_2$ for the remaining fraction, with $\alpha=0.05$, $\theta_1=0.05$, and $\theta_2=10\theta_1$. In this way, $C_k(t)$ is evaluated. Next, in order to obtain $C_{k+1}(t)$ the input signal is defined as $\tilde{x}_{k+1}(t)=\tilde{x}_k(t)-C_k(t)$, and the whole procedure continues until the mode $C_L(t)$ shows no apparent variation. For every point in time the phases $\phi_{EMD}^{(k)}(t)$ are then defined using Hilbert transforms of each mode $C_k(t)$. The frequencies $\omega_{EMD}^{(k)}$ are obtained by averaging the instantaneous frequencies $d\phi_{EMD}^{(k)}/dt$, separately for each mode. Although the instantaneous frequency of each mode can vary in time, by definition the fast oscillations present in the signal are in general extracted into the lower and the slow oscillations into the higher modes so that $\omega_{EMD}^{(0)} > \omega_{EMD}^{(1)} > \cdots > \omega_{EMD}^{(L)}$. Moreover, the mode amplitudes usually decay fast with k so that the signal can be decomposed into a small number of empirical modes. In this approach, the system is characterized by the intrinsic frequency spectrum $\omega_{EMD}^{(k)}$, $k=0,1,\ldots,L$.

Examples of the lowest EMD modes obtained from the variable $x(t)$ of the Lorenz system versus their Hilbert transforms are shown in Fig. 3. In contrast with the original variable $x(t)$ it can be seen that the empirical modes are in fact proper rotations with unique centers and directions of rotation. The average frequencies of the empirical modes are given in Table I. Although it is not always possible to find connection between the consecutive empirical modes and the physical processes underlying the signal under study or its characteristic features [17], it is interesting to compare the results obtained from the EMD and PSS methods for the Lorenz oscillator. Since the $C_0(t)$ mode in general captures the fastest oscillations present in the system, it is tempting to identify it with the fastest rotations of the trajectory around the symmetric unstable foci characterized by the frequency $\omega_{PSS}^{(0)}$. Similarly, the higher modes capturing slower oscillations may be associated with the less frequent jumps between the symmetric parts of the Lorenz attractor characterized by the frequencies $\omega_{PSS}^{(j)}$, $j=1,2,\ldots$. However, an inspection of Table I shows that the corresponding frequencies from the EMD and PSS methods systematically deviate. Thus there is no direct correspondence between the fast oscillations and slower jumps in $x(t)$, which can be distinguished using the geometric approach based on the PSS, and the empirical modes obtained solely from the signal, without any prior knowledge of the geometry of the chaotic attractor. Nevertheless, in the case of the Lorenz oscillator both approaches show that multiple spectral components with distinct frequencies are present in the dynamics of the system and the whole complexity of its oscillations cannot be captured by only one frequency, as suggested by the MV method.

B. Chen system

The Chen system [12] $\dot{x}=\sigma(y-x)$, $\dot{y}=(\sigma-r-z)x+ry$, $\dot{z}=xy-bz$, with $\sigma=35$, $b=3$, and $r=28$, has a chaotic attractor with more complex topology than that of the Lorenz system (Fig. 4). For the Chen oscillator no transformation of variables is known, resulting in a phase trajectory rotating around a unique center point; in particular, the u-z transformation of Sec. II A is not useful for this purpose. Hence, the frequency and phase for the Chen system can be obtained only from the PSS and EMD methods.

Let us start with the PSS method. In contrast with the Lorenz system, the phase trajectory of the Chen system cannot be easily decomposed into fast rotations around unique rotation centers on each of the two symmetric parts of the attractor with $x<0$ and $x>0$ and jumps between these parts. After a large rotation the phase trajectory can perform a series of smaller loops, which can end in another large rotation on the same or the other part of the attractor. The small loops are distributed over a wide interval of the z variable (Fig. 4). Hence, if the PSS is set as $z=r-1$, the resulting frequency distribution $\rho(\omega_i)$, obtained as in Sec. II B, is not unimodal

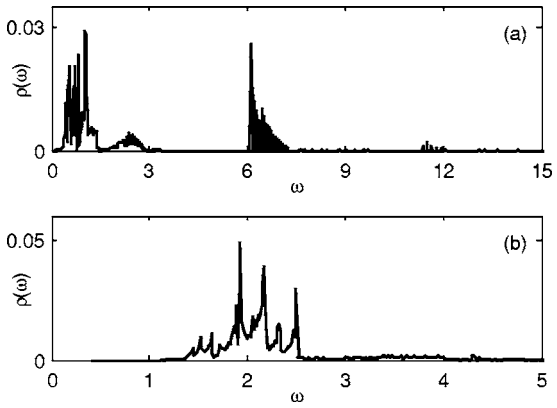

FIG. 5. Frequency distributions $\rho(\omega_i)$ of the uncoupled Chen oscillator with $\sigma=35$, $b=3$, and $r=28$. The surface of section is conditioned by (a) $z=r-1$ and (b) $x=0$.

[Fig. 5(a)], and the same is true if the PSS is shifted along the z axis over a wide interval within the attractor limits. Defining the frequency $\omega_{PSS}^{(0)}$ as the mean over the whole distribution $\rho(\omega_i)$ or a part of it is problematic; thus, the PSS method does not yield unambiguously the basic frequency of the Chen oscillator. If the PSS is set as $x=0$, the frequency distribution exhibits multiple peaks [Fig. 5(b)], related both to the jumps between the two parts of the attractor and to smaller loops performed by the phase trajectory. However, in contrast with the Lorenz system [Fig. 2(b)] these peaks, though distinct, are superimposed on a broad frequency background and the frequency spectrum $\omega_{PSS}^{(j)}$, $j=1,2\ldots$, cannot be easily evaluated by averaging $\rho(\omega_i)$ over separate maxima. Thus, the PSS method shows only qualitatively the existence of the multiple spectral components in the dynamics of the Chen oscillator. In contrast, the EMD method allows decomposition of the $x(t)$ variable into a number of empirical modes with distinct average frequencies $\omega_{EMD}^{(0)} > \omega_{EMD}^{(1)} > \cdots > \omega_{EMD}^{(L)}$ (Table II).

III. APPLICATION OF EMPIRICAL MODE DECOMPOSITION TO THE STUDY OF PHASE SYNCHRONIZATION BETWEEN COUPLED COMPLEX CHAOTIC OSCILLATORS

A. Phase synchronization between parametrically different Lorenz oscillators

In the study of PS, each oscillator is usually characterized by a single phase and frequency. In the synchronized state the phase difference between the oscillators is bounded and the frequency difference is zero [7], or at least close to zero [20]. In contrast, in this paper each oscillator is characterized by its frequency spectrum obtained using the EMD method, and the transition to PS is basically analyzed as a process of merging of the frequencies of the corresponding modes as the coupling strength is increased.

TABLE II. Frequencies for the (uncoupled) Chen system with $\sigma=35$, $b=3$, and $r=28$, obtained using the EMD method (for explanation of symbols see text).

j	$\omega_{EMD}^{(j)}$	j	$\omega_{EMD}^{(j)}$
0	1.87	4	0.19
1	0.96	5	0.11
2	0.55	6	0.06
3	0.32		

The first system under study consists of two parametrically different Lorenz oscillators coupled according to a drive-response scheme,

$$\dot{x}_d = \sigma(y_d - x_d),$$

$$\dot{y}_d = r_d x_d - y_d - x_d z_d,$$

$$\dot{z}_d = x_d y_d - b z_d,$$

$$\dot{x}_r = \sigma(y_r - x_r) + \varepsilon(x_d - x_r),$$

$$\dot{y}_r = r_r x_r - y_r - x_r z_r,$$

$$\dot{z}_r = x_r y_r - b z_r, \tag{1}$$

with $\sigma=10$, $b=8/3$, and, in general, $r_d \neq r_r$. Using the MV method to determine the phase in the response oscillator is inconvenient, because the attractor is modified with changing the parameters σ, r, b, or ε, and, as a result, the center of rotation (u_p, z_p) is shifted accordingly. In contrast, the EMD method makes it possible to observe and describe quantitatively PS in systems with a set of saddle cycles [18]. For this purpose, the phases $\phi_{EMD}^{(d,k)}(t)$ and $\phi_{EMD}^{(r,k)}(t)$ and frequencies $\omega_{EMD}^{(d,k)}$, $\omega_{EMD}^{(r,k)}$, $k=0,1,\ldots,L$, are evaluated from the variables $x_d(t)$ and $x_r(t)$, separately for the drive (d) and response (r) oscillators, for every point in time and for the consecutive modes $C_{d,k}(t)$ and $C_{r,k}(t)$. The parameters r_d and r_r are chosen so that for zero coupling and for each k there is $|\omega_{EMD}^{(d,k)} - \omega_{EMD}^{(r,k)}| \ll |\omega_{EMD}^{(d,k)} - \omega_{EMD}^{(r,k\pm1)}|$; thus, the modes from the drive and response signals with the same index k can be treated as corresponding ones.

In the following the analysis of PS using EMD is constrained to the lowest (most significant) modes with the highest amplitudes. For higher modes, with significantly smaller amplitudes, qualitatively similar scenarios of the transition to PS with increasing coupling strength were observed. A quantitative description of PS using the EMD is based on the study of the adjustment of frequencies of the corresponding modes of the drive and response systems with the increase of ε (frequency entrainment). In Figs. 6(a)–6(c), this process is illustrated for the lowest modes with the fastest intrinsic frequencies.

If $r_d=r_r$, numerical simulations show that the frequencies of all modes of the response system adjust to those of the corresponding modes of the drive system at the same coupling $\varepsilon=7.25$ [Figs. 6(a)–6(c)]. The transition to PS is distinct, and above the transition point the frequencies of the corresponding modes are equal. Above this point complete synchronization between the two Lorenz oscillators occurs; i.e., the trajectories of the two coupled systems merge. Hence, for identical oscillators the transition to PS takes

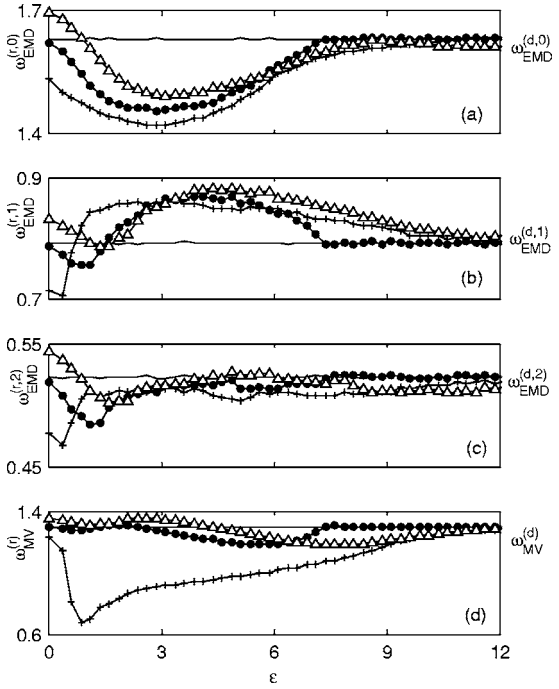

FIG. 6. (a)–(c) Frequencies $\omega_{EMD}^{(d,k)}$ and $\omega_{EMD}^{(r,k)}$ of the lowest empirical modes of the Lorenz drive (lines) and response (lines with symbols) oscillators in Eq. (1) vs the coupling strength ε: (a) $k=0$ mode, (b) $k=1$ mode, and (c) $k=2$ mode. (d) Frequencies $\omega_{MV}^{(d)}$ and $\omega_{MV}^{(r)}$ of the same oscillators vs the coupling strength ε; in all cases, $r_d=27$, $r_r=25$ (+) $r_r=27$ (●), and $r_r=29$ (△).

place simultaneously for all empirical modes and is equivalent to transition to complete synchronization. As a result, PS between empirical modes cannot be observed before the amplitudes of the system variables become correlated.

In contrast, for $r_d \neq r_r$ the frequencies of the corresponding modes are not exactly equal even at high coupling. In this case PS is imperfect, with small, but nonzero differences between the frequencies of the corresponding modes. This resembles imperfect PS between the Lorenz system and periodic forcing [20]. In general, perfect PS between periodic forcing and complex chaotic oscillators with a broad distribution of intrinsic frequencies cannot be reached. Probably, the same is true for PS between corresponding empirical modes of the coupled complex chaotic oscillators, whose instantaneous frequencies are also relatively broadly distributed.

Moreover, the imperfect adjustment of the frequencies of different corresponding modes of the two systems occurs independently, at a different coupling strength. This can be seen, e.g., in Figs. 6(a)–6(c) for $r_d=27$ and $r_r=29$: $\omega_{EMD}^{(r,0)}$ is almost equal to $\omega_{EMD}^{(d,0)}$ ca. for $\varepsilon>8.5$, and $\omega_{EMD}^{(r,2)}$ is almost equal to $\omega_{EMD}^{(d,2)}$ ca. for $4<\varepsilon<8$, while $\omega_{EMD}^{(r,1)}$ is not adjusted to $\omega_{EMD}^{(d,1)}$ ca. for $\varepsilon<10.5$. Hence, for parametrically different oscillators the transition to an imperfectly synchronized state takes place independently for different pairs of corresponding modes. A related observation of the phase locking between certain pairs of corresponding empirical modes, with other pairs exhibiting only intermittent PS or no apparent synchronization, has been reported for coupled, parametrically different chaotic forced van der Pol oscillators [18].

The study of the relationship between PS and generalized synchronization between different chaotic oscillators is difficult, because PS is imperfect and there is no distinct transition from the nonzero to zero frequency difference between corresponding modes. Nevertheless, numerical simulations show that this relationship need not be universal. In the case of generalized synchronization the phase trajectories of the coupled systems do not merge, but a one-to-one function mapping the points of the trajectory of the drive system on those of the response system exists, which can be detected using the auxiliary system approach [5]. It was verified that for $r_d=27$ and, e.g., $r_r=25$ the transition to generalized synchronization between the two Lorenz systems is distinct and occurs at $\varepsilon=8.5$. This is simultaneously or slightly before the frequencies of the modes $C_{d,0}$ and $C_{r,0}$ approximately merge [Fig. 6(a)]. On the other hand, for $r_r=29$ generalized synchronization appears at $\varepsilon=10.5$, after the state of imperfect PS between the $k=0$ modes is established. It is well known that for parametrically different Rössler oscillators, depending on the topological properties of the attractors of the coupled systems, PS can occur before or after generalized synchronization [23]. Also for coupled essentially different chaotic oscillators generalized synchronization usually precedes PS [8]. Thus, the relationship between the generalized synchronization and PS defined on the basis of the EMD method deserves further investigation.

Note that with increasing ε the frequency difference between the corresponding modes of the drive and response systems can rise before PS occurs at strong coupling [Figs. 6(a) and 6(b)]. This phenomenon is analogous to anomalous PS found in coupled chaotic oscillators using different definitions of the phase [8,19]. Anomalous synchronization between the corresponding modes occurs even if $r_d=r_r$, when the mode frequencies in the uncoupled oscillators are equal. This is in contrast with the case of coupled identical Rössler oscillators, where PS appears always, for any coupling [7].

In Fig. 6(d) the dependence of the frequency $\omega_{MV}^{(r)}$ of the response system on the coupling strength is shown for comparison. As mentioned above, the frequency evaluated from the MV method is approximate due to the changes in the attractor of the response system introduced by coupling it to the drive. In particular, this is the reason for a rapid decrease of $\omega_{MV}^{(r)}$ for small coupling in the case of $r_r=25$. Nevertheless, the results of the study of PS between the parametrically different Lorenz systems based on the MV method show many analogies with those obtained using the EMD method. For $r_d=r_r$—i.e., for identical drive and response systems—the MV method reveals the occurrence of PS at $\varepsilon=7.25$, where the frequencies $\omega_{MV}^{(r)}$ and $\omega_{MV}^{(d)}$ become equal, exactly at the threshold for complete synchronization, where also PS between all empirical modes occurs. For $r_d \neq r_r$, even for strong coupling, the frequencies $\omega_{MV}^{(r)}$ and $\omega_{MV}^{(d)}$ are again at most approximately equal and only imperfect PS is observed. Anomalous PS can be also seen in Fig. 6(d), both in the cases of identical and in parametrically different Lorenz systems, though for slightly different ranges of the coupling strength than anomalous PS between the corresponding empirical modes.

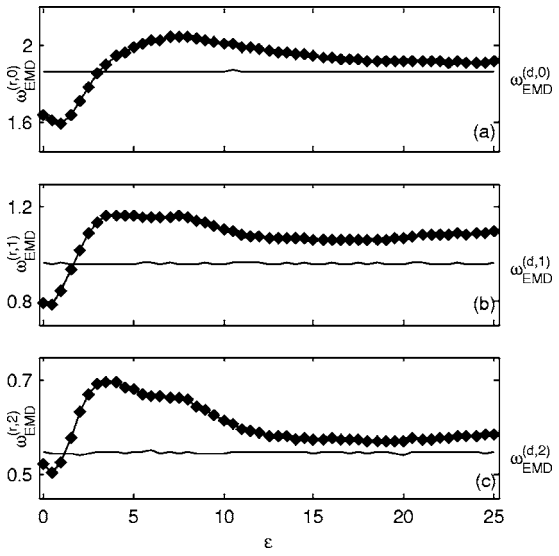

FIG. 7. (a)–(c) Frequencies $\omega_{EMD}^{(d,k)}$ and $\omega_{EMD}^{(r,k)}$ of the lowest empirical modes of the Chen drive (lines) and Lorenz response (lines with symbols) oscillators in Eq. (2) vs the coupling strength ε: (a) $k=0$ mode, (b) $k=1$ mode, and (c) $k=2$ mode.

B. Phase synchronization between essentially different complex chaotic oscillators

The second system under study consists of two coupled essentially different oscillators (i.e., oscillators with topologically different attractors): the Chen oscillator acting as a drive (d) for the Lorenz response (r) oscillator,

$$\dot{x}_d = \sigma_d(y_d - x_d),$$

$$\dot{y}_d = (r_d - \sigma_d - z)x_d + r_d y_d,$$

$$\dot{z}_d = x_d y_d - b_d z_d,$$

$$\dot{x}_r = \sigma_r(y_r - x_r) + \varepsilon(x_d - x_r),$$

$$\dot{y}_r = r_r x_r - y_r - x_r z_r,$$

$$\dot{z}_r = x_r y_r - b_r z_r, \tag{2}$$

with $\sigma_d=35$, $b_d=3$, $r_d=28$, $\sigma_r=10$, $b_r=8/3$, and $r_r=27$. In Fig. 7 the dependence of the frequencies of the lowest empirical modes of the Lorenz oscillator on the coupling strength is shown. For $\varepsilon=0$ the frequencies $\omega_{EMD}^{(d,k)}$ and $\omega_{EMD}^{(r,k)}$, $k=0,1,2$, are close to each other (Fig. 7); thus, the modes $C_{d,k}(t)$, $C_{r,k}(t)$ of the drive (Chen) and response (Lorenz) oscillator with the same index k are corresponding modes. With increasing coupling the frequencies of the corresponding modes can merge, though they usually do not become equal and only imperfect PS is established [Figs. 7(a)–7(c)]. PS occurs separately for different pairs of the corresponding modes; e.g., the modes $C_{d,1}(t)$ and $C_{r,1}(t)$ do not show even imperfect PS for any ε [Fig. 7(b)], in contrast with the $k=0$ and $k=2$ modes, whose frequencies are relatively close for strong coupling. Hence, the definition of PS between complex chaotic oscillators as a process of merging of the frequencies of the corresponding empirical modes with the rise of the coupling strength can be extended to the case of coupled essentially different oscillators. Also anomalous synchronization between the corresponding modes can be observed in this case [Figs. 7(a)–7(c)].

IV. CONCLUSIONS

EMD is an instrument for determining the phase and frequency and its application in this field has many advantages. In this paper the relationship between the EMD method and the well known MV and PSS methods for determining the phase and frequency of the complex chaotic oscillators was investigated. The MV method is applicable only in the case of the Lorenz system and characterizes the oscillator with a single frequency. In contrast, both the PSS and the EMD methods unveil the presence of several spectral components with different frequencies in the dynamics of the complex oscillators. However, the peaks in the frequency distribution obtained using the PSS method, corresponding to the intrinsic frequencies, are separate only in the case of the Lorenz system. In the case of the Chen system, whose attractor has more complex topology, these peaks are superimposed on the broad frequency background; moreover, the PSS method does not yield unambiguously the basic frequency of the Chen oscillator. In contrast, the EMD method always enables decomposition of the chaotic signal into a set of spectral components (modes) with distinct frequencies.

Application of EMD in the investigation of PS between complex chaotic oscillators looks promising. The EMD method enables description of PS not only in terms of merging of the average frequencies of the coupled oscillators, but also in terms of merging of the frequencies of their empirical modes with increasing coupling. The transition to PS can appear independently between different pairs of the corresponding empirical modes, for different ranges of the coupling strength, both in the case of parametrically and in essentially different drive and response systems. The established synchronized state is usually that of imperfect PS, with small but nonzero differences between the frequencies of the corresponding modes. Other interesting phenomena—e.g., anomalous PS between the corresponding modes—can also occur. EMD is a signal-based method and does not require any knowledge of the investigated system or the chaotic attractor. Hence, it is frequently used in the analysis of empirical data [18,24], where it can become widely applicable in the quest of PS between experimentally measured time series.

ACKNOWLEDGMENTS

The authors thank Dr. J. Kurzyna and Professor J. J. Żebrowski for helpful discussions. This work was supported by internal funds of the Faculty of Physics, Warsaw University of Technology, under Grant No. 503 G 1050 0015 000.

[1] A. Pikovsky, M. Rosenblum, and J. Kurths, *Synchronization: A Universal Concept in Nonlinear Sciences* (Cambridge Universiy Press, Cambridge, England, 2003).
[2] S. Boccaletti, J. Kurths, G. Osipov, D. L. Valladares, and C. S. Zhou, Phys. Rep. **366**, 1 (2002).
[3] R. Roy and K. S. Thornburg, Jr., Phys. Rev. Lett. **72**, 2009 (1994).
[4] M. G. Rosenblum, A. S. Pikovsky, and J. Kurths, Phys. Rev. Lett. **78**, 4193 (1997).
[5] N. F. Rulkov, M. M. Sushchik, L. S. Tsimring, and H. D. I. Abarbanel, Phys. Rev. E **51**, 980 (1995).
[6] M. A. Matías, J. Güémez, and C. Martín, Phys. Lett. A **226**, 264 (1997).
[7] M. G. Rosenblum, A. S. Pikovsky, and J. Kurths, Phys. Rev. Lett. **76**, 1804 (1996).
[8] Shuguang Guan, C.-H. Lai, and G. W. Wei, Phys. Rev. E **72**, 016205 (2005).
[9] A. Pikovsky, M. Zaks, M. Rosenblum, G. Osipov, and J. Kurths, Chaos **7**, 680 (1997).
[10] E. Rosa, E. Ott, and M. H. Hess, Phys. Rev. Lett. **80**, 1642 (1998).
[11] E. N. Lorenz, J. Atmos. Sci. **20**, 130 (1963).
[12] G. Chen and T. Ueta, Int. J. Bifurcation Chaos Appl. Sci. Eng. **9**, 1465 (1999).
[13] J. H. Lü, G. Chen, and D. Z. Cheng, Int. J. Bifurcation Chaos Appl. Sci. Eng. **14**, 1507 (2004).
[14] V. S. Anishchenko, A. N. Silchenko, and I. A. Khovanov, Phys. Rev. E **57**, 316 (1998).
[15] A. S. Pikovsky, M. G. Rosenblum, G. V. Osipov, and J. Kurths, Physica D **104**, 219 (1997).
[16] E.-H. Park, M. A. Zaks, and J. Kurths, Phys. Rev. E **60**, 6627 (1999).
[17] N. E. Huang *et al.*, Proc. R. Soc. London, Ser. A **454**, 903 (1998).
[18] M. Chavez, C. Adam, V. Navarro, S. Boccaletti, and J. Martineire, Chaos **15**, 023904 (2005).
[19] B. Blasius, E. Montbrió, and J. Kurths, Phys. Rev. E **67**, 035204(R) (2003).
[20] M. A. Zaks, Eun-Hyoung Park, M. G. Rosenblum, and J. Kurths, Phys. Rev. Lett. **82**, 4228 (1999); Eun-Hyoung Park, M. A. Zaks, and J. Kurths, Phys. Rev. E **60**, 6627 (1999).
[21] T. Yalcinkaya and Y.-C. Lai, Phys. Rev. Lett. **79**, 3885 (1997).
[22] G. Rilling, P. Flandrin, and P. Goncalves (unpublished).
[23] G. V. Osipov, Bambi Hu, Changsong Zhou, M. V. Ivanchenko, and J. Kurths, Phys. Rev. Lett. **91**, 024101 (2003).
[24] M. A. Bray and J. P. Wikswo, Phys. Rev. E **65**, 051902 (2002); I. M. Jánosi and R. Müller, *ibid.* **71**, 056126 (2005).